J Mater Sci: Mater Med (2006) 17:1113–1125
DOI 10.1007/s10856-006-0538-3

The properties of biomimetically processed calcium phosphate on bioactive ceramics and their response on bone cells

M. Vaahtio · T. Peltola · T. Hentunen · H. Ylänen · S. Areva · J. Wolke · J. I. Salonen

Received: 1 April 2005 / Accepted: 24 October 2005

Abstract This study looks for grounds to alter the chemical composition (phosphate, calcium, silica and carbonate), dissolution properties, structure and nanotopography of the biomimetically processed surfaces on bioactive ceramics to optimize their shown ability to influence bone cell behaviour and production of new bone. In the bone environment desirable characteristic of these materials is their ability to be remodeled by natural osteoclastic resorption. Different silica and carbonate containing calcium phosphate layers were prepared on bioactive glasses 9 (S53P4) and 1-98 (S53P2) and sol-gel processed pure silica SiO_2 in C- and R-SBF (conventional and revised simulated body fluid) for varying periods of time. It was shown that in R-SBF the CaP layer formed faster compared to C-SBF. The CaP layer in the R-SBF contained more carbonate (CO_3^{2-}) compared to that formed with the same immersion time in C-SBF. The CaP so formed in R-SBF with faster precipitation is more amorphous than the bonelike HCA formed in C-SBF. The results indicate that the most suitable surface for both osteoblasts and osteoclasts was found to be an amorphous CaP having mesoporous nanotopography and proper dissolution rate of calcium and silica.

M. Vaahtio · T. Peltola
Turku Biomaterials Centre, University of Turku, Itäinen Pitkäkatu 4B, FIN-20520 Turku, Finland, and Department of Prosthetic Dentistry and Biomaterials Science, Institute of Dentistry, University of Turku, Lemminkäisenkatu 2, FIN-20520 Turku, Finland

T. Hentunen
Department of Anatomy, Institute of Biomedicine, University of Turku, Kiinamyllynkatu 10, FIN-20520 Turku, Finland

H. Ylänen
Process Chemistry Centre, Åbo Akademi University, Piispankatu 8, FIN-20500 Turku, Finland

S. Areva
Turku Biomaterials Centre, University of Turku, Itäinen Pitkäkatu 4B, FIN-20520 Turku, Finland, and Department of Physical Chemistry, Åbo Akademi University, Porthaninkatu 3-5, FIN-20500 Turku, Finland

J. Wolke
Department of Periodontology and Biomaterials, College of Dental Science, University Medical Center Nijmegen, P. O. Box 9100, 6500 HB Nijmegen, The Netherlands

J. I. Salonen
Turku Biomaterials Centre, University of Turku, Itäinen Pitkäkatu 4B, FIN-20520 Turku, Finland

M. Vaahtio (✉)
University of Turku, Turku Biomaterials Centre, Itäinen Pitkäkatu 4B, FIN-20520 Turku, Finland,
e-mail: minna.vaahtio@utu.fi

Introduction

When melted bioactive glasses [1–7] and sol-gel derived bioactive ceramics [8–11] are implanted *in vivo*, a hydroxyapatite (HCA) layer, similar to that of the mineral of bone, is formed on the surface of the material. It is believed that the prerequisite for glasses and ceramics to bond to living bone is the formation of a layer of carbonate containing hydroxyapatite on the materials surface [12–13]. Furthermore, the influences of different surface characteristics of bioactive glasses and CaP ceramics on adhesion and proliferation properties of osteoblasts have been widely studied. A known fact is that the surface roughness (on micro-meter scale) and surface reactivity of the bioactive ceramics has an effect on cell attachment, proliferation, differentiation and mineralization of bone cells [14–15]. In addition, some studies show that there are specific nanodimensions between 1–100 nm that have a direct influence either on the adsorption of proteins

(e.g., vitronectin) [16] that are important with respect to adhesion and growth of osteoblasts and endothelial cells or on the gene activation of fibroblasts [16–19]. In our previous studies we found also that the sol-gel derived TiO_2-coatings contain a lot of "surface pores" at dimensions of 15–50 nm. These dimensions promote the formation of bone mineral-like calcium phosphate as well as attachment to hard and soft tissues, although a thick CaP layer is not formed [20–23]. In recent studies also the importance of the dissolving ionic products of the Bioglass 45S5 on the osteoblast proliferation and differentiation has been shown [24–26]. It was suggested that relatively high steady state silicon concentration (10–20 ppm) in cell culture (or in tissue) induces osteoblast proliferation and differentiation [26]. Although the significance of Ca in the bone mineralisation process is well-known, the ability of extracellular Ca to regulate cell specific responses has recently only been demonstrated [27]. In addition, it has been shown that lower inorganic phosphate content in bioactive glasses favors osteoblast differentiation [28]. Furthermore, also the surface pH seems to have an influence on cellular activity [29–30].

The current trend in biomaterial research is to design materials that will help the body's own healing and regenerative processes. In bone repair, recent studies have focused on materials that could be remodeled by osteoclastic resorption and subsequently would be replaced by newly formed bone through osteoblastic activity [31]. Redey *et al.* suggested that osteoclastic resorption may be limited to the solubility of the biomaterial [32]. Best resorption activity was obtained using calcium carbonate as a substrate. In addition to the solubility, surface energy plays an essential role in osteoclast adhesion, whereas osteoclast spreading may depend on the surface chemistry, especially on protein adsorption or formed CaP layer. It has also been shown that carbonated apatite is superior to other apatites or calcium phosphates as a bioresorbable bone substitute, which leads to normal osteoclastic resorption [33–34]. Furthermore, Langstaff *et al*. found that silicon-stabilized microporous calcium phosphate ceramics are insoluble in biological fluid but are resorbed when acted upon by osteoclasts [35–36]. Also the effect of particle size on macrophage differentiation, osteoclast differentiation and bone resorption has been studied [37–38]. It was found that osteoclast formation is not significantly influenced by particle size (0.1, 1, 10 and 100 μm) and it was suggested that particles derived from uncemented HA are likely to induce less osteoclast formation than cemented HA. However, the reason for this behaviour was not discussed.

To study the bioactivity of biomaterials or to produce biomimetic CaP coating *in vitro*, a simulated body fluid (conventional SBF (C-SBF)) was developed for more than ten years ago [39–40]. The fluid contains all essential inorganic constituents found in human plasma. The only difference is the lower concentration of HCO_3^- and higher concentration of Cl^- compared to those of human plasma. Oyane *et al*. [41] has introduced a series of renewed SBFs and among them was the R-SBF (revised simulated body fluid) [42]. In the R-SBF, the concentrations of HCO_3^- and Cl^- have been changed to equal levels to that in human plasma. Thus, the biomimetic CaP coatings produced in various SBFs provide the possibility to create CaP layers with different chemical composition and dissolution properties. Therefore, the biomimetically produced CaP layers have been used to study the influence of the surface properties on bone cell response. Although, the osteoblast responses have been widely studied [14, 29, 43] in respect of CaP layer properties such studies on osteoclastic response are still lacking.

The objective of this study was to prepare and characterize different silica and carbonate containing calcium phosphate surfaces. The CaP precipitates were formed on bioactive glasses (glass 9 and 1-98) and on mesoporous sol-gel derived silica during immersion in C-SBF and R-SBF for varying periods of time. The structure and chemical composition of the biomimetically processed CaP layers was studied by a scanning electron microscope equipped with energy dispersive X-ray (SEM-EDX), fourier transform infrared spectroscopy (FTIR), X-ray photoelectron spectroscopy (XPS), atomic force microscopy (AFM) and a thin-film X-ray diffractometer (TF-XRD). The dissolution properties of the ionic species from the produced CaP layers were studied using a tris buffer solution. The osteoblast and osteoclast activities were determined using the specific alkaline phosphatase (ALP) [44] and tartrate-resistant acid phosphatase (TRACP 5b) [45] assays, respectively.

Materials and methods

Preparation of specimens (Glass 9 and 1-98, sol-gel-derived SiO_2 monoliths)

For the manufacturing of the bioactive glasses (glass 9 (S53P4) and 1-98 (S53P2)), a standard method was used [46]. Table 1 gives the composition of the glasses. The final cast of the bioactive glasses was made to a form of a quadrangular bar (11 × 11 mm). From the bar, discs (2 mm thick) were sawn using a diamond precision saw (Buehler Isomet 5000, Lake Bluff, IL, USA). The surfaces of the discs were polished using fine paper and water.

Table 1 Compositions of the studied glasses in oxide weight-% of the glass

	SiO_2	CaO	Na_2O	P_2O_5	K_2O	MgO	B_2O_3
Glass 9	53	20	23	4			
Glass 1-98	53	22	6	2	11	5	1

Table 2 Composition [mM] of the C-SBF, R-SBF and human plasma

Ion	C-SBF	R-SBF	Plasma
Na^+	142.0	142.0	142.0
K^+	5.0	5.0	5.0
Mg^{2+}	1.5	1.5	1.5
Ca^{2+}	2.5	2.5	2.5
Cl^-	147.8	103.0	103.0
HCO_3^-	4.2	27.0	27.0
HPO_4^{2-}	1.0	1.0	1.0
SO_4^{2-}	0.5	0.5	0.5

A pure silica gel was prepared from tetraethylortosilicate (TEOS), deionized water, polyethyleneglycol (PEG; MW∼10,000) and nitric acid as a catalyst. PEG (0.70 g) was dissolved in deionized water (8.00 g). A constant molar ratio of the silica sol was $TEOS:H_2O:HNO_3 = 1:15:2.9$. The silica sol was pipetted into round plastic moulds (1 ml/mould) that were tightly closed and kept at 40°C and 40% relative humidity for gelation, aging and drying. After gelation (18 h) the holes were made to the caps of moulds. The gel specimens were dried for 9 days and then heat-treated at 500°C (10°C/h from 25°C to 500°C → 2 h at 500°C → slow cooling to room temperature) to porous monoliths. Porous silica monoliths were round with a diameter of approximately 12 mm and a thickness of 2 mm weighing about 120 mg.

Biomimetic preparation of CaP layers

The polished glass specimens and the SiO_2 specimens were immersed in two different SBFs, a conventional C-SBF and a revised R-SBF. The composition of the SBFs is given in Table 2. The glass specimens were immersed in 6 mL and the SiO_2 specimens in 50 mL of SBF in closed polyethylene test tubes. The ratio of surface area (SA) to SBF solution volume (V) was for glasses 0.4 cm^{-1} and for SiO_2 specimens 0.06 cm^{-1}. All the test tubes were placed in a shaking water bath at 37°C (Comfort Heto Master Shake, SBD 50 BIO). The glass specimens were immersed in either of the SBFs for 6, 12, 24, 48, 96, and 168 h. The respective time periods for sol-gel derived SiO_2 specimens were 12, 48, 96, 168, 240, and 336 h. After immersion, the glass specimens were rinsed and kept in ethanol before the analyses. The SiO_2 specimens were washed in deionized water, dried at 40°C and 40% relative humidity (1–3 days) and in a desiccator (4–7 days) to a constant weight and sterilized for 2 h at 170°C. The sterilized SiO_2 specimens were stored in the desiccator before the analyses.

SBF tests and ion concentration analysis

The silica dissolution and the calcium phosphate formation ability of the specimens were studied using two different SBFs that were prepared as described above. Three pieces of each specimen were used to investigate the reactions of glasses 9 and 1-98 and pure SiO_2 in the SBFs. Each glass specimen was immersed in 6 ml and SiO_2 specimen was immersed in 50 ml of C-SBF or R-SBF in a polyethylene test tube covered with a tight lid. Three samples of both SBFs enclosed in test tubes without a specimen were used as controls to examine solutions stability. The glass specimens were immersed in the SBF solutions for 7 days and SiO_2 specimens for 14 days. The test tubes were placed in a shaking water bath at a constant temperature of 37°C.

The silica dissolution of the specimens was determined by measuring the silicon released into the SBF. Sample solutions were monitored for silicon, phosphorus and calcium concentrations as a function of immersion time. Silicon and phosphorus concentrations were measured separately by two different Molybdenum blue methods with an UV-Vis spectrophotometer (Shimadzu UV-1601). The silicon measurement was based on reduction of 1-amino-2-naphthol–4-sulfonic acid [47] and the phosphorous was determined by Lowry-Lopez method [48]. Calcium concentrations were determined with spectrophotometer as an o-cresolphtalein complex at A_{570} (Microplate reader, Multiskan EX, type 355) [49]. Three parallel measurements were done for all the sample solutions at each time point.

SEM-EDX analysis

The morphology and the chemical composition of the surface of the specimens were examined using a scanning electron microscope (SEM, LEO 1530, Cambridge, England) equipped with a energy dispersive X-ray analyzer (EDXA, Thermo Noran 2226A-1 SES-SN, Waltham, MA, USA). The surfaces of the specimens were sputtered with carbon for the SEM-EDX monitoring.

FTIR

Infrared adsorption measurements were carried out using Fourier transform infrared spectroscopy (FTIR, Spectrum One, Instrument serial number 52434, Perkin Elmer, Beaconsfield, England) and a diffuse reflectance unit (DRIFT, accessory serial number 181296, Perkin Elmer, Beaconsfield, England). Spectra in the region 4000-450 cm^{-1} were recorded using potassium bromide as a background material. The resolutions of the FTIR measurements were 2 cm^{-1}.

XPS

The chemical nature of the outermost surface of the specimens was obtained by X-ray photoelectron spectroscopy (XPS, Perkin-Elmer PHI 5400 ESCA System Spectrometer).

The XPS measurements were performed at a base pressure of 1×10^{-8} Torr using Mg Kα X-ray ($\lambda = 1253.6$ eV) source. The electron analyzer pass energy in the XPS high-resolution scans was 89.45 eV and the grazing angle of the photoelectrons was 45°. The UNIFITTU (version 2.1) software was used for peak fitting and quantitative chemical analysis. The high-resolution spectra were charge compensated by setting the binding energy (BE) of the C 1s contamination peak to 284.6 eV.

TF-XRD

Specimens were subjected to X-Ray diffraction (XRD) analysis on a thin-film Philips X-Ray Diffractometer (PW 3710) using CuKα-radiation. The diffractometer was operated at 40 kV, 40 mA with a scanning speed of 0.013°/s at 2θ-steps of 0.020°. The angle of incident beam was 2.5°.

Specimens' dissolution after biomimetic process

The dissolution of the different reaction layers formed on the surface of the bioactive specimens during biomimetic processes was studied using a tris buffer (pH 7.4, 37°C) as a dissolution medium. The volume of the solution was 25 mL. At each sampling interval, 6 mL of sample solution was withdrawn and replaced immediately with an identical volume of fresh medium. Three parallel samples were examined. Sample solutions were monitored for silicon, phosphorus and calcium concentrations as described above.

Osteoblast growth

Human osteosarcoma Saos-2 cells were used in this study, although these cells can not form bone. However, these cells are osteoblastic and we were studying their growth characteristics only. Saos-2 cells (4×10^4) were grown on SBF treated and untreated glasses 9 and 1-98, and SiO_2 material in the culture medium (α-minimal essential medium (α-MEM) + 10% fetal calf serum (FCS)) for 4 days. Six parallel glass specimens were used. At the end of the test, the culture medium was removed and the cells were lysed with a lysis buffer (50 mM Tris-HCl, 0.1% Triton X-100, pH 7.6). Then the cell lysates were frozen (−20°C) over night and thawed. ALP/protein were used as an osteoblast marker, which showed the growth of osteoblastic cells on different biomaterials [50]. ALP activity was determined colorimetrically using pNPP as a substrate at pH 9.7. The total protein content was analyzed with the protein assay (Bio-Rad Laboratories). ALP activity levels varied from culture to culture. In order to compare the results between the experiments we adjusted the specific ALP activity in the control to 100 and the other results were multiplied by this coefficient. The results were expressed as ALP activity/mg protein (% of control).

Osteoclast survival

Long bones (femur and tibia) from 1-to 2-day-old rat pups were dissected and the osteoclasts were scraped into α-minimal essential medium (α-MEM) containing 10% fetal calf serum (FCS). The preparation contained highly active osteoclasts and marrow stromal cells [51, 52]. Stromal cells were essential, because they supported osteoclast activity by expressing growth factors, such as RANKL, on their surface. Cell suspension (50 μl/specimen) was pipetted carefully onto the specimens (SBF treated and untreated glasses) that were in a 24-well culture plate (1 ml medium/well). Six parallel glass specimens were used. Osteoclasts were cultured for 4 days. At the end of the culture, the media were collected and the cells were detached by adding 0.2 ml of lysis buffer (10 mM Tris-HCl, pH 7.4, 300 mM NaCl, 0.5% Triton X-100, 1 mM EGTA, 1 mM PMSF) into the wells. Samples were frozen (−20°C). Alatalo *et al.* have shown before that TRACP 5b activity in the culture correlates with the number of osteoclasts. TRACP 5b/mg protein was determined from the lyzed cells using immunoassay with anti-TRACP antibody prepared in rabbits [45]. First, TRACP of the specimen was bound to the well plate, and its enzyme activity was detected colorimetrically using p-nitrofenylphosphate (pNPP) as a substrate at pH 5.7. The protein content in the cell lysate was analyzed with a protein assay (Bio-Rad Laboratories). First of all, in this assay we measured osteoclast survival on the biomaterials. When osteoclasts undergo into apoptosis, they detach from the biomaterial surface. We measured TRACP 5b from the survived cells after lysing the cells with a detergent. Also for the osteoclasts, the specific TRACP-5b activity was calculated as a relative osteoclast activity. The results were expressed as TRACP 5b activity/mg protein (% of control).

AFM

The surface topography and roughness of the specimens was determined by the non-contact tapping mode atomic force microscopy (AFM) using a NanoScope III multimode AFM (Digital Instruments, Santa Barbara, CA) apparatus. The line profiles (3 specimens of each material surface) obtained from the image analysis software of the microscope was analyzed more closely for the topography of the materials by image analysis utilizing a CAD program (Rhinoceros Beta).

Results

SBF tests and ion concentration analysis

The amount of dissolved silica was nearly equal for both glasses in C-SBF (Fig. 1A). However, in C-SBF approx. twice the amount of silica is dissolved from the glass 9 compared to that in R-SBF. Also for the glass 1-98 the amount of released silica in R-SBF is lower than in C-SBF. The constant level of released silica was achieved after 4 days of immersion in C- and R-SBF for the glass 9 (95 ppm and 47 ppm) and for the glass 1-98 (95 ppm and 68 ppm). The dissolution profiles of silica were quite similar for the pure SiO_2 specimens in both SBFs.

In general, the faster reactivity (CaP formation ability) was obtained for all studied materials after immersion in R-SBF than in C-SBF as evidenced by the decreasing phosphorus concentration (Fig. 1B). Similar trend was observed in the Ca concentration analysis (not shown). The CaP formation started within 12 h for the glasses 9 and 1-98 immersed in R-SBF and within 24 h immersed in C-SBF.

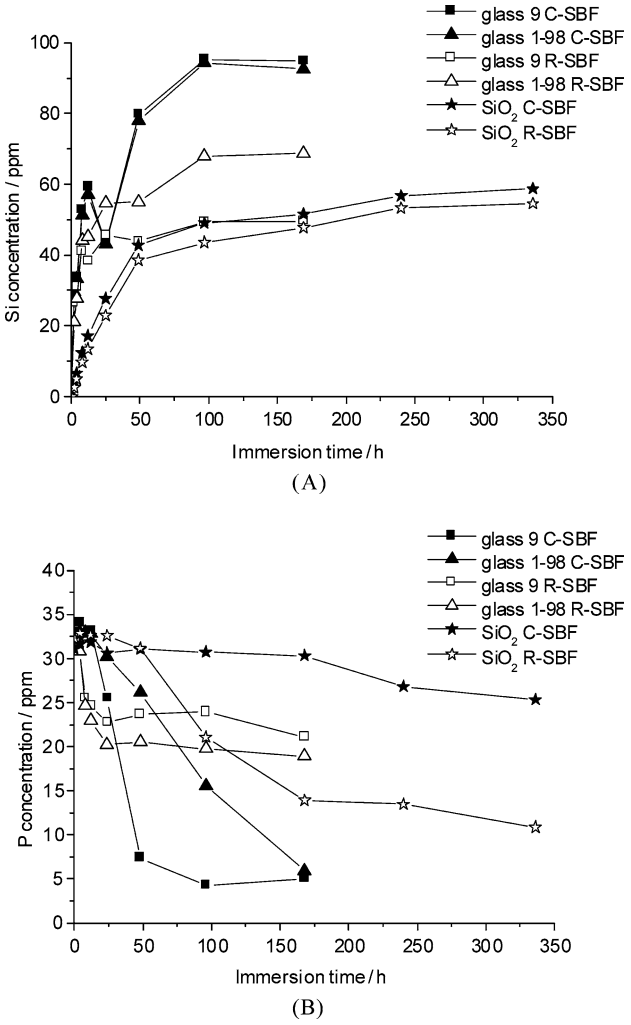

Fig. 1 (A) Silicon concentrations of glass 9, glass 1-98 and sol-gel derived SiO_2 as a function of immersion time in C-SBF and R-SBF. (B) Phosphorus concentrations of glass 9, glass 1-98 and sol-gel derived SiO_2 as a function of immersion time in C-SBF and R-SBF.

SEM-EDX analysis

Similarly to the solution analysis, the EDX analysis showed (as evidenced by the decrease in the relative amount of silica as a function of time) that the CaP layer grew on glass 9 significantly slower in C-SBF than in R-SBF (Fig. 2). The reaction layers were dominated by calcium and phosphorus after 48 h and 12 h in C-SBF and R-SBF treated glasses, respectively. Although the glass 1-98 reacted slower than glass 9, similar trend was observed for the C-SBF and R-SBF treatments, respectively (Fig. 2). Elemental compositions of the reaction layers of the sol-gel-derived SiO_2 specimens immersed in C- and R-SBF showed that the CaP layer was formed after 168 h of immersion in C-SBF and after 96 h of immersion in R-SBF (Fig. 2) having similar elemental compositions with the C-SBF treated glass 1-98 (12 h and 24 h) and glass 9 (6 h) surfaces.

FTIR

In addition to the SEM-EDX analysis further information of the molecular composition of the formed CaP layer was provided by FTIR measurement, especially for identification of carbonate [53]. The CaP layers on both glasses were difficult to analyze due to the disturbing effect of glass substrates itself. However, the carbonate bands were visible earlier in the R-SBF than in the C-SBF. For the glass 9 carbonate bands become visible after 6 h immersion in R-SBF and after 96 h immersion in C-SBF (not shown). For the glass 1-98 carbonate bands become visible after 6 h immersion in R-SBF and after 168 h immersion in C-SBF (not shown).

XPS

Because FTIR analysis did not give any quantitative results for carbonate, further information of the elemental composition of the outermost calcium phosphate surface layer was obtained by the XPS analysis (Fig. 3). Carbonate (C1s: CO_3-C) peak was detected having binding energy (BE) of ~289 eV. The amount of carbonate was found to increase as a function of increasing Ca/P ratio. The Ca/P ratios approx. 1.15 and 1.4 corresponds to the literature values for amorphous and crystalline CaP phases, respectively [54–55]. In addition, the amount of carbonate was found to reach its maximum value already after 6 h of immersion in R-SBF, whereas in C-SBF the equal carbonate amount was observed only after 168 h of immersion.

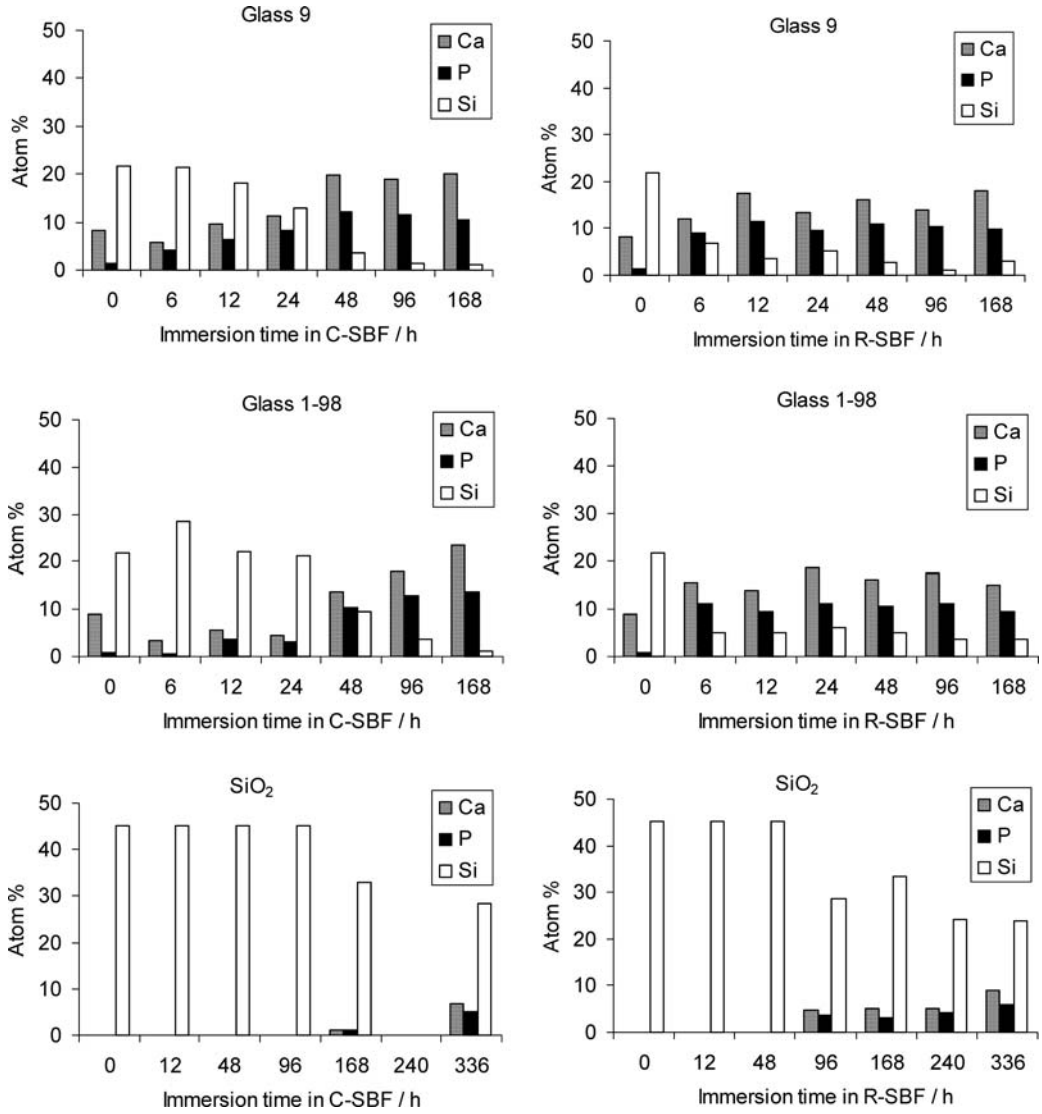

Fig. 2 The elemental compositions (obtained by EDX) of the reaction layers of the test specimens as a function of immersion time in C- and R-SBF.

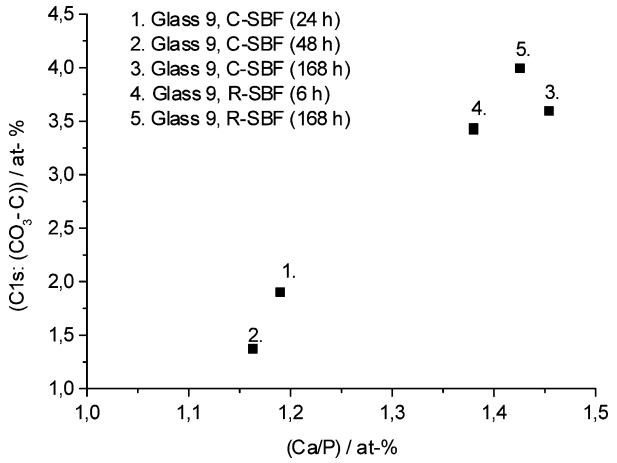

Fig. 3 Relative atomic percentages of carbonate (obtained by XPS) as a function of Ca/P ratio.

TF-XRD

The crystal structure of the formed CaP layer was determined by TF-XRD measurement. The XRD patterns for the glass 9 immersed in C-SBF and R-SBF showed reflections resulting from poorly crystalline bone-like HCA only after 168 h of immersion (Figs. 4(A) and (B)). However, the HCA is less crystalline in the sample immersed in R-SBF, in addition, the formed CaP phases in both SBFs were not as crystalline as the reference bone powder. The glass 1-98 immersed in C-SBF and R-SBF showed no evidence of a crystalline phase (not shown). There were also some crystalline HCA present in the sol-gel derived SiO_2 sample immersed in C-SBF for 336 h (not shown).

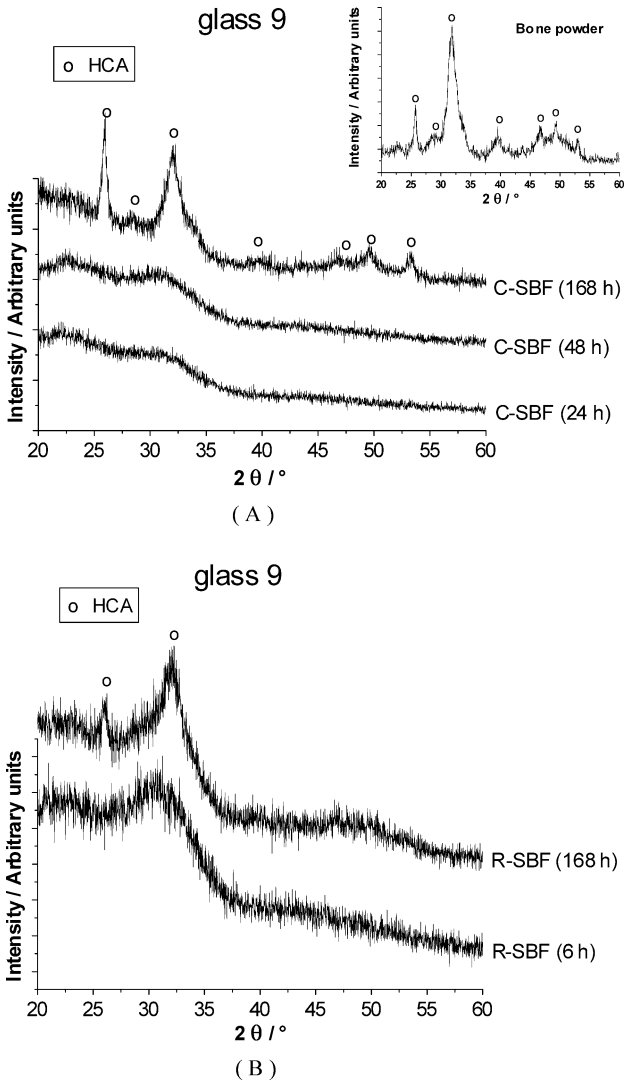

Fig. 4 XRD patterns of the surfaces of (A) glass 9 immersed in C-SBF and (B) in R-SBF as a function of time. The XRD pattern of bone powder is given as a reference.

Specimens dissolution after biomimetic process

The dissolution of the specimens after the biomimetic treatment in SBFs was studied in tris buffer solution. The dissolution rates (ppm/h) were calculated from the linear portion of the original dissolution curves. Especially, for the glass specimens a general trend was seen. The longer the immersion times in SBFs, the lower the silica dissolution rates (Fig. 5). Thus, the formed CaP layer significantly hindered the silica dissolution from the substrate glasses. The dissolution rate of calcium decreased gradually after 24 h immersion in both SBFs. The dissolution rate of phosphorus was approximately equal regardless of the immersion time in both SBFs. In addition, the dissolution rates of silica, calcium and phosphorus are slightly lower for the glass 1-98 than those for the glass 9. In contrast to the glass specimens, the CaP layer formed on sol-gel derived SiO_2 specimens did not have significant influence on the release of silica (Fig. 5). The calcium and phosphorus dissolution rates from the SiO_2 specimens immersed either in C-SBF or in R-SBF were quite low.

Osteoblast growth

In general, osteoblasts grew well on all the SBF treated and untreated glass 9 and 1-98 specimens (Fig. 6). For all glasses (except R-SBF treated glass 9) the control specimen gave the highest osteoblast activity. As shown in Fig. 7, the sol-gel-derived SiO_2 specimen gave the highest ALP activity and was two-fold higher than in the bioactive glasses. However, the SBF treated sol-gel-derived glasses gave very low ALP activity. Otherwise there were no significant differences in osteoblast activities between the specimens.

Osteoclast survival

The osteoclastic activity as measured by the specific TRACP 5b activity (Fig. 8) is expressed as relative TRACP 5b activity (Fig. 9). The TRACP 5b activity of the C-SBF treated (24 h) glass 9 was almost 3-fold compared to other specimens. For the R-SBF treated glass 9 the TRACP 5b activity increased gradually until 96 h immersion time point. The glass immersed for 168 h gave almost the same activity as the control glass. The highest TRACP 5b activity was obtained for the glass 9 immersed for 24 h in C-SBF or 96 h in R-SBF (TRACP 5b activity was 2-fold compared to control). For the glass 1-98, there were no significant differences in the TRACP 5b activities between C- and R-SBF treated or untreated specimens. However, short immersion time in C-SBF (6 h, 12 h and 24 h) and in R-SBF (48 h) gave lower TRACP 5b activities than the other SBF treated 1-98 glass specimens. In addition, the osteoclast response was not obtained for the SBF treated sol-gel-derived glasses due to difficulties in culture preparation.

AFM

The C-SBF treated glass 9 (24 h) and glass 1-98 (48 h) surfaces that had quite similar elemental compositions but different dissolution properties or the C-SBF treated glass 9 (24 h) and the R-SBF treated glass 9 (96 h) that had the highest osteoclast survival properties were analyzed in detail with AFM. The peak distance distribution, describing the "surface pore size" distribution, for the C-SBF treated glass 9 (24 h) surface was between 5-50 nm, having median and mean values of 28 and 38 nm, respectively (Fig. 10). The glass 1-98 (48 h) surface is smoother and the peak distance distribution is wider (Fig. 10) than in the glass 9. Nearly all of the peak distances appear to be between 5-110 nm, having median and mean value of 43 and 58 nm, respectively. In addition, for the

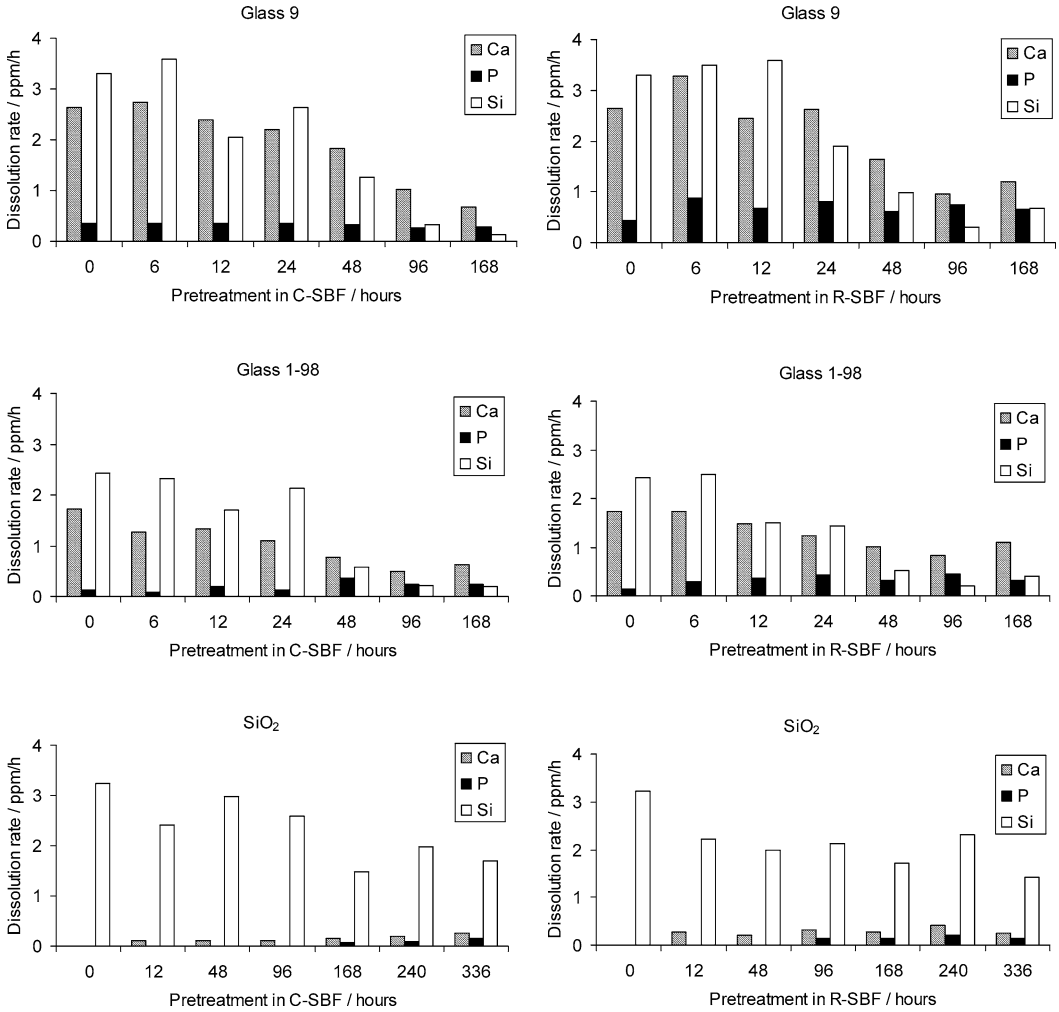

Fig. 5 The dissolution of calcium, phosphorus and silicon from the C- and R-SBF treated specimens in tris buffer. The dissolution rate was calculated from the linear portion of the original dissolution curve.

R-SBF treated glass 9 (96 h) (Fig. 10) the surface topography was nearly similar (surface pore size 5–50 nm, median value 24 nm and mean value 27 nm) with the C-SBF treated glass 9 (24 h).

Discussion

The current study looked for grounds to alter the chemical composition (phosphate, calcium, silicon and carbonate), dissolution properties, structure and nanotopography of the biomimetically processed surfaces on bioactive ceramics to optimize their shown ability to influence bone cell behaviour and production of new bone. The objective of this study was to prepare and characterize different silica and carbonate containing calcium phosphate surfaces. The CaP surfaces were prepared using a conventional C-SBF and a revised R-SBF. The SBF, EDX and FTIR results showed that reactions occurred fastest on glass 9 surface and slowest on pure silica surface (Figs. 1 and 2). In addition, also the presence of soluble calcium and phosphate (increases supersaturation of SBF) in glasses decreases the CaP formation time compared to pure silica where mainly the materials surface characteristics control the heterogenous nucleation and CaP formation. The reactions were faster in R-SBF compared to C-SBF for all studied materials. This finding is inconsistent with the results of a recent study of Zhang *et al.* [56]. According to their results, the studied phosphate free glass reacted slower in R-SBF compared to C-SBF. Furthermore, they found that during the immersion of the phosphate free glass in R-SBF, calcite ($CaCO_3$) was formed on the glass surface. The formation of calcite in R-SBF can be explained by its six-fold concentration of HCO_3^- compared to C-SBF (Table 2). However, in our study no calcite was found on any of the surfaces. As expected, the CaP layers formed in R-SBF was found to contain more CO_3^{2-} than the CaP layers formed in C-SBF (Fig. 3). Theoretically, immersion of bioactive material in the R-SBF should result in the formation of bone like HCA due to the increased amount of CO_3^{2-}. However, TF-XRD measurements showed clearly that the CaP layers

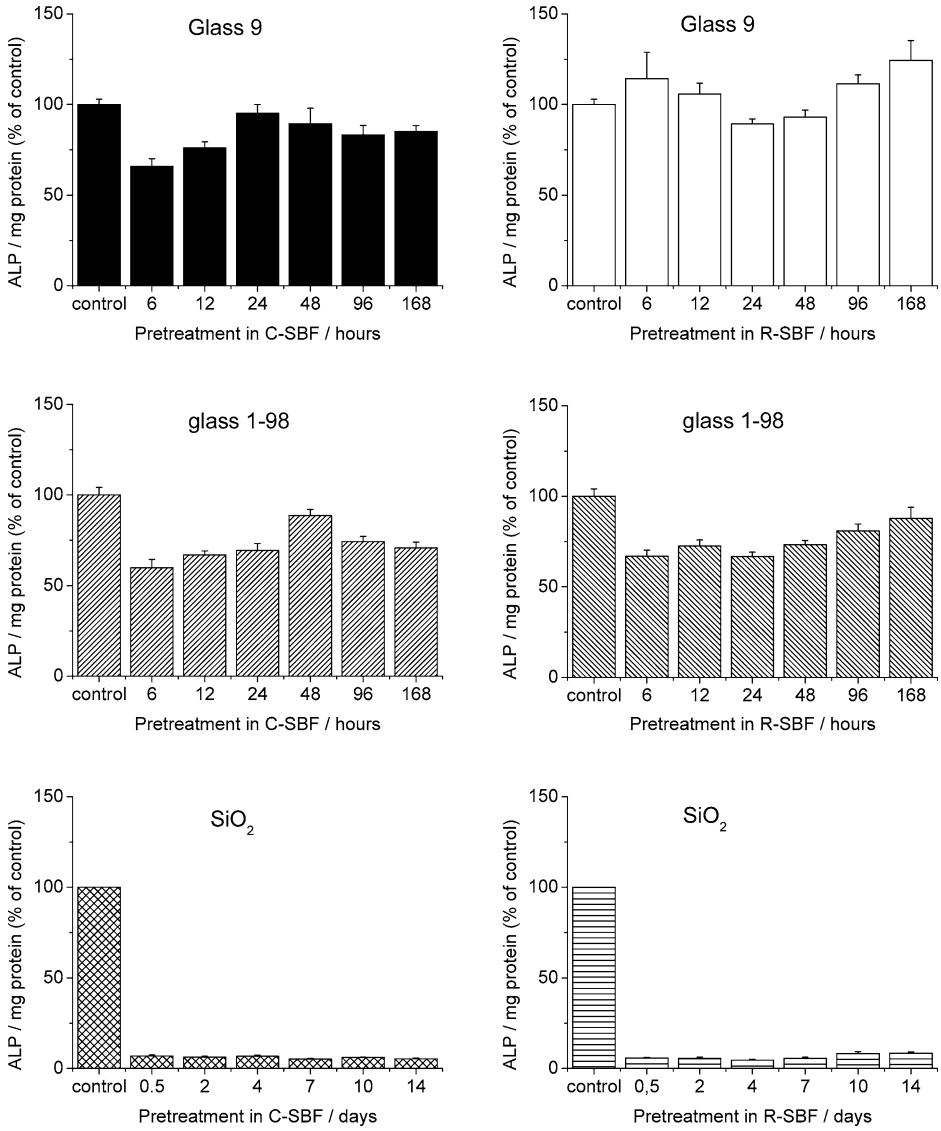

Fig. 6 ALP activities on glass 9, glass 1-98 and sol-gel-derived SiO_2 after four days in culture. Specimens were pretreated in C-SBF and R-SBF for varying periods of time.

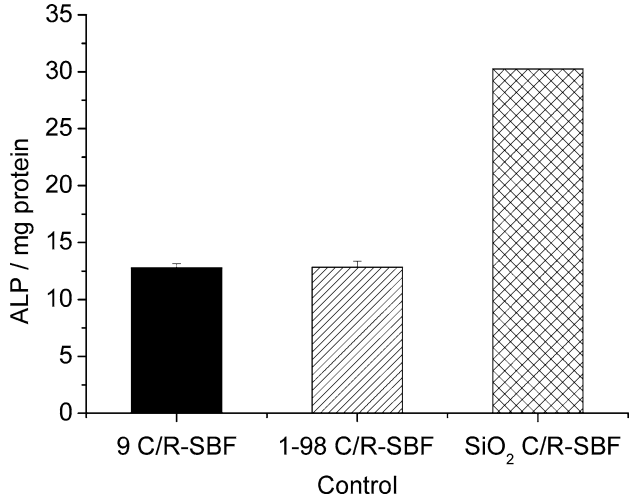

Fig. 7 Growth of SaOs-2 cells on control (untreated) glass specimens in different cultures. The results are expressed as ALP activity/mg protein (% of control).

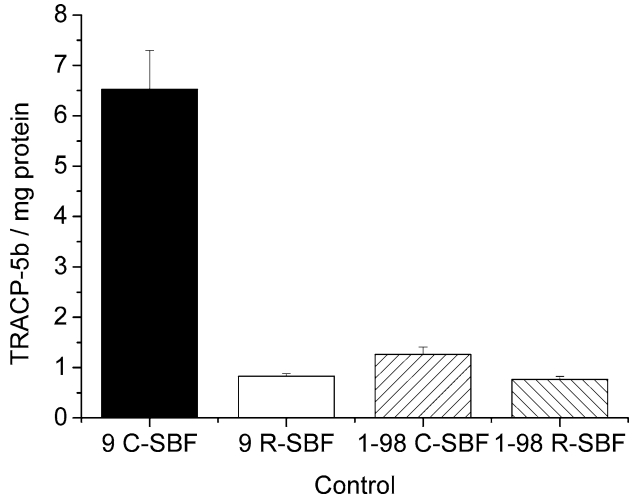

Fig. 8 Survival of primary rat osteoclasts on control (untreated) glass specimens in different cultures. The results are expressed as TRACP-5b/mg protein (% of control).

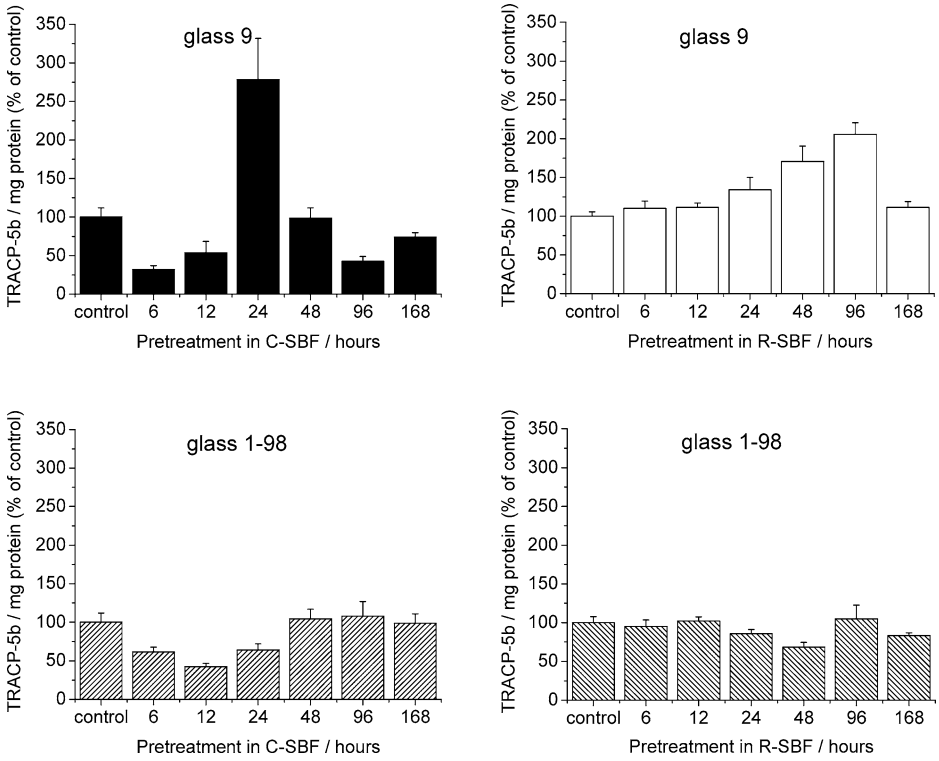

Fig. 9 TRACP-5b activities on glass 9 and glass 1-98. Specimens were pretreated in C-SBF and R-SBF for varying periods of time.

formed in C-SBF were more crystalline than the CaP layers formed in R-SBF (Figs. 4(A) and 4(B)) and resembled to that of carbonated hydroxyapatite (HCA) as the immersion time increases. The reason may be the observed instability of the R-SBF solution, which was also shown by Oyane *et al.* [57].

The dissolution tests in tris buffer showed that, in general, the longer the immersion times in SBFs, the lower the silica dissolution rates in both SBFs (Fig. 5). This is explained by the fact that during the immersion in SBF the CaP layer grows thicker and becomes more dense and crystalline as the immersion time increases. It is obvious that the denser and thicker CaP layer blocks the dissolving ions from the substrate materials more effectively than thinner CaP layers. This is more evident in the bioactive glass samples than in the pure sol-gel derived SiO_2 materials. This indicates that although the formed CaP layers were "dense" for both of these materials the underlying sol-gel material still shows high reactivity and silica dissolution as compared to the SBF treated bioactive glass specimens.

The osteoblast activity was high for all SBF treated or untreated glass 9 and 1-98 specimens (Fig. 6). Cells on control glasses (also sol-gel derived) gave the highest activities, except for the glass 9, where cells on some R-SBF treated surfaces gave slightly better results than the control glass. This is in contrast to the result reported by Olmo *et al.* [43], where they showed that the biomimetically produced CaP layer significantly increased the osteoblast activity (by 1.7 fold). However, this difference can result from the slight differences in the reactivity of the used glasses. Although the sol-gel derived SiO_2 treated with SBF showed almost no osteoblast activity, the pure sol-gel SiO_2 showed even higher activity than the bioactive glass specimens (Fig. 7). To date, no reports exist where pure SiO_2 materials express better osteoblast activity than calcium and phosphate containing bioactive glasses. The reason for this is still unclear and needs to be verified. Nevertheless, this might indicate that the dissolving silica ions could be more important to bone-cell activation than the formation of CaP on materials surface. This is partly in agreement with Xynos *et al*. where the importance of dissolving silica on osteoblast activition has been shown [24–26].

It has been suggested earlier [33, 34] that biomimetic CaP coatings on bioactive material having variable compositions in terms of solubility and carbonate content would affect the osteoclastic response. In this study, the highest osteoclast survival was observed for the C-SBF treated glass 9 (24 h), which showed three-fold higher survival than the other studied specimens (statistically significant, $p < 0.05$). In addition, for the R-SBF treated glass 9 it was shown that osteoclast survival was statistically higher as the immersion time was increased up to 96 h *i.e.* the carbonate content of the CaP layer increases. However, for the most crystalline CaP layer having also the highest content of carbonate the osteoclast survival decreased to the same level as in the control glass. These results are in contrast to the observations, where

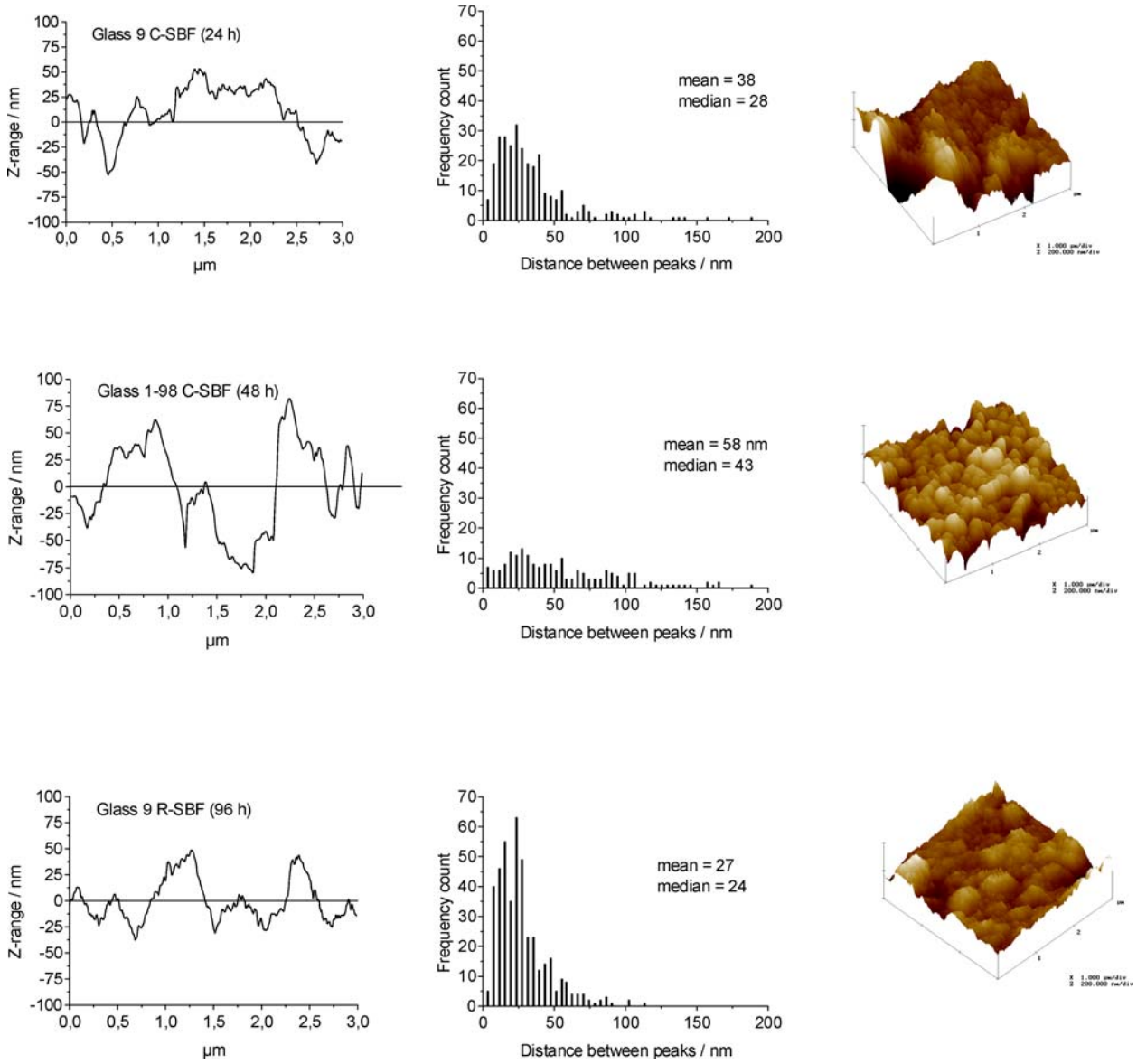

Fig. 10 Line profiles, calculated peak distance histograms and 3D images for the C-SBF immersed (24 h) glass 9, C-SBF immersed (48 h) glass 1-98 and R-SBF immersed (96 h) glass 9.

the increasing amount of carbonate in the CaP layer was found to increase the osteoclastic survival [32–34]. In addition, no clear trends were observed between the solubility and the osteoclastic survival, which is in contrast to earlier report [32]. However, our results suggest that for a good osteoclast survival the surface should rather be an amorphous HCA than crystalline with the appropriate carbonate content. This is in agreement with de Bruijn *et al*. [58]. Thus, the osteoclast survival is not a function of only one material parameter.

Interestingly the C-SBF treated glass 9 (24 h) and glass 1-98 (48 h), which had a similar kind of calcium, phosphorus and silicon balance in the composition as well as similar crystallinity and carbonate amount, had significant differences in the osteoclast survival (Fig. 9). The osteoclast survival is much higher for the glass 9 (24 h) than for the glass 1-98 (48 h). Though the chemical composition is similar, the nanotopography and dissolution properties are different. The silica and calcium solubility is much higher for the glass 9 (24 h) and also most of the surface pores are between 2-50 nm that is different from the glass 1-98 (48 h) (surface is smoother and the peak distance distribution is wider than in the glass 9). Also for the R-SBF treated glass 9 (96 h) having the second highest osteoclast survival had similar topography with the C-SBF treated glass 9 (24 h). These nanodimensions match well with the dimensions shown to be important with respect to adhesion and growth of osteoblasts and fibroblasts [16–23].

Conclusions

The composition and structure of biomimetically processed CaP layers and dissolution properties of bioactive substrates can be modified with wide range by controlling the immersion time and by changing the SBF solution. Additionally, it was shown that amorphous CaP containing silica and carbonate with favourable nanotopography seems to be beneficial for the osteoclast survival. The best osteoclast survival was obtained for the glass 9 immersed 24 h in C-SBF. Also osteoblasts grew well on this surface. However, the pure sol-gel SiO_2 showed the highest osteoblast activity. Thus, this study gives important information about the implant material properties of bioresorbable bioactive ceramic that we should use and develop for osteoclastic resorption.

Acknowledgments The National Technology Agency of Finland (TEKES) is acknowledged for financial support. SA would like to thank the Graduate School of Materials Research for financial support.

References

1. L. HENCH, *J. Am. Ceram. Soc.* **81** (1998) 1705.
2. H. OONISHI, T. SUGIHARA, E. TSUJI, L. HENCH and J. WILSON, in "Bioceramics," edited by R. Z. LeGEROS and J. P. LeGEROS (World Scientific, Singapore, 1998) vol. 11 p. 23.
3. L. HENCH, R. SPLINTER, W. ALLEN and T. GREENLEE, *J. Biomed. Mat. Res. Symp.* **2** (1971) 117.
4. Ö. H. ANDERSSON, K. H. KARLSSON, K. KANGASNIEMI and A. YLI-URPO, *Glastech. Ber.* **61** (1988) 300.
5. O. PEITL FILHO, G. LA TORRE and L. HENCH, *J. Biomed. Mater. Res.* **30** (1996) 509.
6. M. BRINK, *J. Biomed. Mater. Res.* **36** (1997) 109.
7. H. YLÄNEN, T. HELMINEN, A. HELMINEN, J. RANTAKOKKO, K. KARLSSON and H. ARO, *Ann. Chir. Gyn.* **88** (1999) 237.
8. P. LI, in "Ph.D. Thesis" (University of Leiden, Leiden, The Netherlands, 1993).
9. T. PELTOLA, M. JOKINEN, H. RAHIALA, E. LEVÄNEN, J. ROSENHOLM, I. KANGASNIEMI and A. YLI-URPO, *J. Biomed. Mater. Res.* **44** (1999) 12.
10. M. HAMADOUCHE, A. MEUNIER, D. C. GREENSPAN, C. BLANCHAT, J. P. ZHONG, G. P. LA TORRE and L. SEDEL, *J. Biomed. Mater. Res.* **54** (2001) 560.
11. C. J. BRINKER and G. W. SCHERER, in "Sol-Gel Science" (Academic Press INC., San Diego, 1990).
12. L. HENCH, *J. Am. Ceram. Soc.* **74** (1991) 1487.
13. T. KOKUBO, *Biomaterials* **12** (1991) 155.
14. P. DUCHEYNE and Q. QIU, *Biomaterials* **20** (1999) 2287.
15. K. MATSUZAKA, X. F. WALBOOMERS, M. YOSHINARI, T. INOUE and J. A. JANSEN, *Biomaterials* **24** (2003) 2711.
16. T. J. WEBSTER, C. ERGUN, R. H. DOREMUS, R. W. SIEGEL and R. BIZIOS, *J. Biomed. Mater. Res.* **51** (2000) 475.
17. M. J. DALBY, M. O. RIEHLE, H. JOHNSTONE, S. AFFROSSMAN and A. S. G. CURTIS, *Biomaterials* **23** (2002) 2945.
18. M. J. DALBY, S. J. YARWOOD, M. O. RIEHLE, H. J. H. JOHNSTONE, S. AFFROSSMAN and A. S. G. CURTIS, *Exp. Cell. Res.* **276** (2002) 1.
19. M. J. DALBY, M. O. RIEHLE, D. S. SUTHERLAND, H. AGHELI and A. S. G. CURTIS, *J. Biomed. Mater. Res.* **69A** (2004) 314.
20. M. JOKINEN, in "Ph.D. thesis" (Åbo Akademi University, Turku, 1999).
21. T. PELTOLA, in "Ph.D. thesis" (Turun yliopisto, Turku, 2000).
22. T. PELTOLA, H. PALDAN, N. MORITZ, S. AREVA, J. KORVENTAUSTA, M. JOKINEN, T. NÄRHI, R. HAPPONEN and A. YLI-URPO, *Key. Eng. Mat.* **218–220** (2002) 207.
23. S. AREVA, H. PALDAN, T. PELTOLA, T. NÄRHI, M. JOKINEN and M. LINDEN, *J. Biomed. Mater. Res.* **70A** (2004) 169.
24. I. D. XYNOS, A. J. EDGAR, L. D. K. BUTTERY, L. L. HENCH and J. M. POLAK, *Biochem. Biophys. Res. Commun.* **276** (2000) 461.
25. I. D. XYNOS, A. J. EDGAR, L. D. K. BUTTERY, L. L. HENCH and J. M. POLAK, *J. Biomed. Mater. Res.* **55** (2001) 151.
26. L. L. HENCH, *Key. Eng. Mat.* **192–195** (2001) 575.
27. T. YAMAGUCHI, N. CHATTOPADHYAY, O. KIFOR, R. R. BUTTERS, Jr. T. SUGIMOTO and E. M. BROWN, *J. Bone. Miner. Res.* **13** (1998) 1530.
28. S. LOSSDÖRFER, Z. SCHWARTZ, C. H. LOHMANN, D. C. GREENSPAN, D. M. RANLY and B. D. BOYAN, *Biomaterials* **25** (2004) 2547.
29. A. EL-GHANNAM, P. DUCHEYNE and I. M. SHAPIRO, *Biomaterials* **18** (1997) 295.
30. Y. JOSSET, F. NASRALLAH, E. JALLOT, M. LORENZATO, O. DUFOUR-MALLET, G. BALOSSIER and D. LAURENT-MAQUIN, *J. Biomed. Mater. Res.* **67A** (2003) 1205.
31. A. F. SCHILLING, W. LINHART, S. FILKE, M. GEBAUER, T. SCHINKE, J. M. RUEGER and M. AMLING, *Biomaterials* **25** (2004) 3963.
32. S. A. REDEY, S. RAZZOUK, C. REY, D. BERNACHE-ASSOLLANT, G. LEROY, M. NARDIN and G. COURNOT, *J. Biomed. Mater. Res.* **45** (1999) 140.
33. S. LEEUWENBURGH, P. LAYROLLE, F. BARRERE, J. DE BRUIJN, J. SCHOONMAN, C. A. VAN BLITTERSWIJK and K. DE GROOT, *J. Biomed. Mater. Res.* **56** (2001) 208.
34. Y. DOI, H. IWANAGA, T. SHIBUTANI, Y. MORIWAKI and Y. IWAYAMA, *J. Biomed. Mater. Res.* **47** (1999) 424.
35. S. LANGSTAFF, M. SAYER, T. J. N. SMITH and S. M. PUGH, *Biomaterials* **22** (2001) 135.
36. S. LANGSTAFF, M. SAYER, T. J. N. SMITH, S. M. PUGH, S. A. M. HESP and W. T. THOMPSON, *Biomaterials* **20** (1999) 1727.
37. A. SABOKBAR, R. PANDEY and N. A. ATHANASOU, *J. Mater. Sci.: Mater. Med.* **14** (2003) 731.
38. A. SABOKBAR, R. PANDEY, J. DIAZ, J. M. W. QUINN, D. W. MURRAY and N. A. ATHANASOU, *J. Mater. Sci.: Mater. Med.* **12** (2001) 659.
39. T. KOKUBO, H. KUSHITANI, S. SAKKA, T. KITSUGI and T. YAMAMURO, *J. Biomed. Mat. Res.* **24** (1990) 721.
40. P. LI, C. OHTSUKI, T. KOKUBO, K. NAKANISHI, N. SOGA, T. NAKAMURA and T. YAMAMURO, *J. Am. Ceram. Soc.* **75** (1992) 2094.

41. A. OYANE, K. ONUMA, A. ITO, T. FURUYA, H. M. KIM, T. KOKUBO and T. NAKAMURA, *Key. Eng. Mat.* (1998) 218.
42. H. M. KIM, T. MIYAZAKI, T. KOKUBO and T. NAKAMURA, *Key. Eng. Mat.* **192–195** (2001) 47.
43. N. OLMO, A. I. MARTIN, A. J. SALINAS, J. TURNAY, M. VALLET-REGI and M. A. LIZARBE, *Biomaterials* **24** (2003) 3383.
44. J. E. AUBIN and F. LIU, in "Principles of bone biology" (Academic Press, San Diego) p. 51.
45. S. L. ALATALO, J. M. HALLEEN, T. A. HENTUNEN, J. MÖNKKÖNEN and H. K. VÄÄNÄNEN, *Clin. Chem.* **46** (2000) 1751.
46. H. YLÄNEN, K. H. KARLSSON, A. ITÄLÄ and H. T. ARO, *J. Noncryst. Solids.* **275** (2000) 107.
47. O. G. KOCH and G. A. KOCH-DEDIC, in "Handbuch der spureanalyse" (Springer, Berlin, 1974) p. 1105.
48. L. F. LELOIR and C. E. CARDINI, in "Methods of enzymology III" (Academic Press, New York, 1972) p. 840.
49. K. L. CHENG, K. UENO and T. IMAMURA, in "Handbook of organic analytical reagents" (CRC Press INC., Florida, 1982).
50. Q. QU, M. PERÄLÄ-HEAPE, A. KAPANEN, J. DAHLLUND, J. SALO and H. K. VÄÄNÄNEN and P. HÄRKÖNEN, *Bone* **22** (1998) 201.
51. T. R. ARNETT and D. W. DEMPSTER, *Endocrinology* **120** (1987) 602.
52. P. LAKKAKORPI, J. TUUKKANEN, T. HENTUNEN, K. JÄRVELIN and K. VÄÄNÄNEN, *J. Bone. Miner. Res.* **4** (1989) 817.
53. I. REHMAN and W. BONFIELD, *J. Mater. Sci.: Mater. Med.* **8** (1997) 1.
54. C. C. CHUSUEI, D. W. GOODMAN, M. J. VAN STIPDONK, D. R. JUSTES and E. A. SCHWEIKERT, *Anal. Chem.* **71** (1999) 149.
55. S. AREVA, T. PELTOLA, E. SÄILYNOJA, K. LAAJALEHTO, M. LINDEN and J. B. ROSENHOLM, *Chem. Mater.* **14** (2002) 1614.
56. Y. ZHANG, H. TADAKAMA, M. MIZUNO, M. YANAGISAWA and T. KOKUBO, *Ceramic engineering and Science Proceedings* **23(4)** (2002) 789.
57. A. OYANE, K. ONUMA, A. ITO, H. M. KIM, T. KOKUBO and T. NAKAMURA, *J. Biomed. Mater. Res.* **64A** (2003) 339.
58. J. D. DE BRUIJN, Y. P. BOVELL and C. A. VAN BLITTERSWIJK, in "Bioceramics," edited by Ö. H. Andersson and A. Yli-Urpo (Butterworth-Heinemann Ltd., 1994) vol. 7, p. 293.